AJNR

Myoepithelioma of the Parotid Gland: CT Imaging Findings

S. Wang, H. Shi, L. Wang and Q. Yu

Myoepithelioma of the Parotid Gland: CT Imaging Findings

S. Wang
H. Shi
L. Wang
Q. Yu

BACKGROUND AND PURPOSE: Myoepitheliomas (MEs) are rare tumors of the parotid gland. Only a few case reports describing CT imaging features of ME have been published. The aim of this study was to describe and characterize the CT findings of MEs of the parotid gland.

MATERIALS AND METHODS: We retrospectively reviewed CT images of ME with pathologic correlation in 10 cases (4 men and 6 women; age range, 30–70 years) collected between August 2003 and October 2007 from our pathologic database. All of the CT images were retrospectively evaluated with respect to the location, size, marginal morphology, enhancement, and enhancement pattern by 2 experienced radiologists.

RESULTS: Nine tumors were located in the superficial lobe of the parotid gland, and 1 was located in the tail of parotid gland. All of the tumors abut on the capsule of the gland. Nine tumors had well-defined margins with lobulations in 5 patients. Two cases showed homogenous enhancement. In the other 8 cases, the enhancement was inhomogeneous because of enhancing nodules and nonenhancing areas of linear bands, slitlike-shaped or of cystic configuration.

CONCLUSION: CT imaging findings of MEs were well circumscribed, enhancing the mass lesion with smooth or lobulated margins, located chiefly in the superficial lobe and abutted on the capsule of the gland. They may contain enhancing nodules and nonenhancing areas of linear bands, slitlike-shaped or of cystic configuration. Although MEs are a rarity, they should be suspected when a tumor shows all of the characteristics noted here.

Myoepithelioma (ME) is a benign salivary gland tumor composed almost exclusively of sheets, islands, or cords of cells with myoepitheliomal differentiation.[1] MEs account for 1.5% of all of the tumors in the major and minor salivary glands,[2] and 40% arise in the parotid glands.[2] The use of CT for the assessment of parotid tumors is well established. Although much has been written on the CT appearance of the pleomorphic adenomas and Warthin tumors,[3-9] the detailed imaging features of MEs of the parotid gland have not been described previously in the English language literature. In this study, we describe the CT appearance of 10 histologically proven cases of MEs of the parotid gland.

Materials and Methods

Patients

We retrospectively reviewed CT images of MEs with pathologic correlation in 10 cases (3 men and 7 women; age range, 30–70 years; mean age, 47.5 years) collected between August 2003 and October 2007 from our pathologic data base.

CT Imaging Technique

CT images were obtained in LightSpeed-16 (GE Medical Systems, Waukesha, Wis). All of the cases were imaged with 5-mm contiguous section thickness. The images were acquired at 120 kV and 250 mA, with a pitch of 1 mm and a 1-second scan time, followed by reconstruction by using the soft tissue algorithm. Bolus intravenous dose of

70 mL of nonionic contrast (300 mg/mL) was given to all of the 10 patients at the rate of 2.0–2.5 mL/s. Scanning was initiated 40 seconds after the onset of contrast injection. All of the images were available on PACS program, and CT densities were measured on the workstation (GE 4.1).

CT Image Analysis

All of the CT images were retrospectively evaluated with respect to location, size, marginal morphology, enhancement, and enhancement pattern. The tumors were presumed to be enhancing if the attenuation of postcontrast CT scan was 20 Hounsfield units (HUs) more than the precontrast CT scan. The enhancement patterns were divided into homogenous (uniform) and inhomogeneous (nonuniform). The nonhomogenously enhancing tumors could include the enhancing nodules and nonenhancing areas of linear bands, slitlike-shaped or of cystic configuration. The enhancing nodules were defined as 40 HU increased after postcontrast scan and having a round or ovoid shape. A lesion having a central hypoattenuated area with 3 or more thin lines was termed "slitlike-shaped," whereas a "cystic area" was defined as having a CT scan attenuation of 25 HU or less. Two senior qualified head and neck radiologists and 1 pathologist correlated the CT image and pathologic specimen.

Results

CT Imaging Findings

Size, Location, and Marginal Morphology. The average maximal cross-sectional diameter was 1.7 cm (range, 0.90–2.74 cm; Table). Nine tumors were located in the superficial lobe of the parotid gland, and 1 was located in the tail of parotid gland. All of the tumors abut on the capsule of the gland. Nine of the tumors had well-defined margins, and the remaining one had an indistinct margin (Fig 2) because of inflammation. There were lobulated margins in 5 tumors. On CT, a capsulelike low attenuation rim was detected in only 2 tumors.

| Case No.	Size, mm	Margin	Contour	Enhancement	Comments	Microscopic Examination
1	25.0 × 21.3 × 16.4	Well defined	Lobulated	Inhomogeneous	Enhancing nodules, slitlike-shaped	Clearcytoplacytoid, epithelioid, collagenous, hemorrhage
2	13.3 × 8.2 × 12.2	Well defined	Lobulated	Inhomogeneous	Enhancing nodules, linear band	Plasmacytoid, mucoid
3	9.2 × 7.9 × 12.6	Well defined	Smooth	Homogeneous	Enhancing nodules	Spindle, plasmacytoid
4	14.6 × 14.6 × 18.6	Well defined	Lobulated	Inhomogeneous	Enhancing nodules, linear band	Plasmacytoid, mucoid
5	17.3 × 15.7 × 27.1	Well defined	Smooth	Inhomogeneous	Enhancing nodules, slitlike-shaped	Plasmacytoid, mucoid, hemorrhage
6	8.5 × 7.5 × 13.2	Well defined	Lobulated	Inhomogeneous	Enhancing nodules, slitlike-shaped	Plasmacytoid, collagenous, hemorrhage
7	21.6 × 16.4 × 27.4	Well defined	Smooth	Inhomogeneous	Enhancing nodules, cystic area	Spindle, cystis degeneration
8	17.6 × 17.0 × 21.2	Indistinct	Smooth	Inhomogeneous	Enhancing nodules, cystic area, calcification	Infected, plasmacytoid, cystis degeneration
9	13.5 × 15.6 × 18.2	Well defined	Lobulated	Inhomogeneous	Enhancing nodules, cystic area	Epithelioid, cystis degeneration
10	7.2 × 6.6 × 9.3	Well defined	Smooth	Homogeneous	Enhancing nodule	Spindle, plasmacytoid
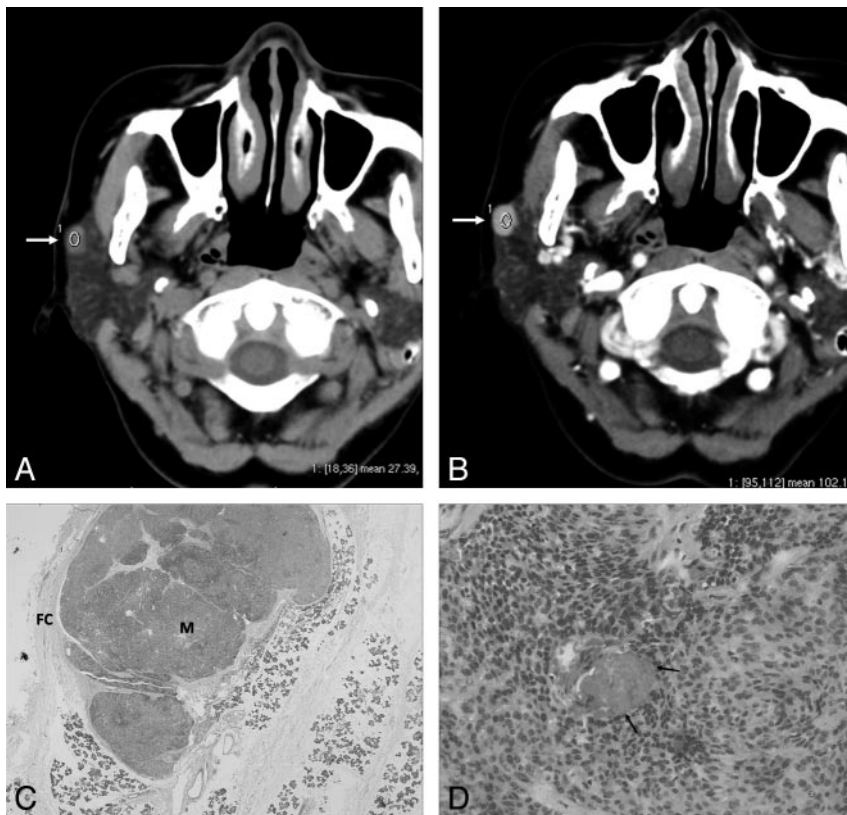
Fig 1. A 62-year-old woman with ME. *A*, Precontrast axial CT scan shows a round, well-defined mass (27.39 HU) in the superficial lobe of the right parotid gland abutting on the capsule of gland (*arrow*). *B*, Contrast-enhanced axial CT scan shows the mass (102.11 HU) with homogeneous strong enhancement (*arrow*). *C*, Microscopic examination (hematoxylin-eosin stain [HE]; ×2) shows that the ME (M) is separated from the parotid gland and the surrounding soft tissues by a fibrous capsule (FC). The stroma is scanty. *D*, Microscopic examination (HE; ×100) shows that the tumor is composed of the plasmacytoid and spindle cells. Relatively large vessels are seen in the tumor (*arrows*).

with plentiful blood vessels (Fig 1). The abundant surrounding stroma, either collagenous or mucoid, were seen in 5 tumors and hemorrhage in 3 of the 6 tumors (Fig 3). Cystic changes were seen in 3 tumors (Fig 2). All of the tumors had a thin fibrous capsule and were well circumscribed, but one was noncircumscribed because of infection (Fig 2).

The immunocytochemistry was detected in 6 of the 10 tumors. The result showed that myoepithelial cells stain positive for cytokeratin, and muscle-specific actin, express S-100 protein, and glial fibrillary acidic protein were positive in all of the tumors.

Enhancement Behavior. All of the tumors were enhanced. The average CT attenuation of precontrast scans was 29.78 HU (range, 23.00–39.00 HU), and the average maximal CT attenuation of postcontrast scan was 108.37 HU (range, 80.00–146.00 HU). The tumor showed homogenous enhancement in 2 cases (20%; Fig 1). The remaining 8 (80%) of the 10 tumors showed inhomogeneous enhancement, with enhancing nodules in 8 tumors, cystic areas in 3 tumors (Fig 2), slitlike-shaped nonenhancing area in 3 tumors (Fig 3), and linear nonenhancing bands in 2 tumors (Fig 4). One tumor showed 2 calcifications (Fig 2).

Pathologic Findings
All of the patients underwent surgery. The histopathologic diagnosis of ME was made in all 10 of the cases (Table). One of the cases was a recurrence. All of the tumors had epithelial nets

Discussion
Benign adenomas account for 65.5% of salivary gland tumors.[10] MEs were recognized as a histologically distinct entity in 1991 by the World Health Organization.[11] An incidence of 1%–7% of all primary salivary gland tumors is often cited.[2] The incidence of 4.68% in our hospital falls within this range.

ME is a benign salivary gland tumor composed almost exclusively of sheets, islands, or cords of cells with myoepithelial differentiation that may exhibit spindle, plasmacytoid, epithelioid, or clear cytoplasmic features.[1] Other terms that have been associated with this tumor include myoepithelial adenoma and benign myoepithelial tumor. The age of patients with ME ranges from 9 to 85 years, with an average of 44 years and the peak age of occurrence in the third decade.[2] It typically presents as a solitary, slowly growing, otherwise asymptomatic mass. MEs develop preferentially in the parotid gland (40%).[2]
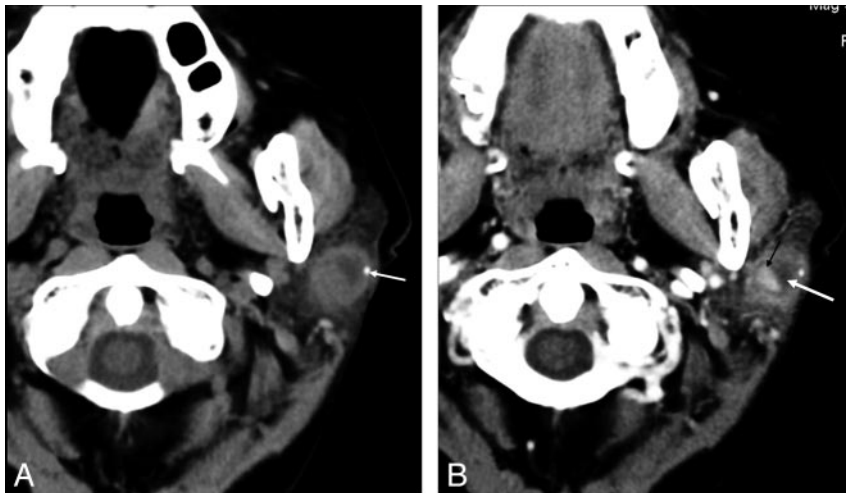
Fig 2. A 66-year-old woman with ME. *A*, Precontrast axial CT scan shows an indistinct margin mass in the superficial lobe of the left parotid gland abutting on the capsule of the gland with calcification (*arrow*). *B*, Contrast-enhanced axial CT scan shows the mass with inhomogeneous enhancement. It contains a central enhancing nodule (*small black arrow*) and a nonenhancing peripheral cystic component (*white arrow*). *C*, Microscopic examination (HE; ×10) shows the epithelioid nest (*arrow*) with a lot of vessels and a cystic component in the center (*black asterisk*). *D*, Microscopic examination (HE; ×20) shows the inflamed cells (*long arrows*) and the tumor cells (*short arrow*).
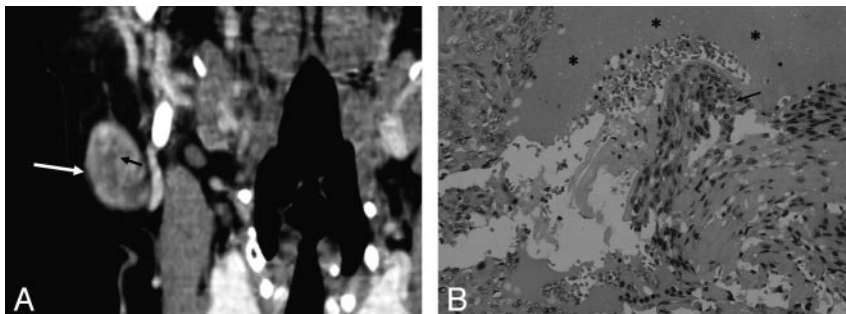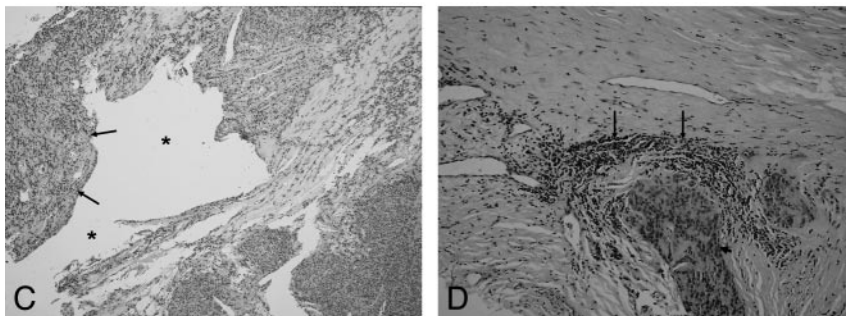
Fig 3. A 56-year-old woman with ME. *A*, Contrast-enhanced multiplanar reformatted coronal CT scan shows a well-defined mass in the tail of the right parotid gland with inhomogeneous enhancement (*white arrow*). Note the slitlike-shaped nonenhancing area (*small black arrow*). *B*, Microscopic examination (HE; ×40) shows that there are hemorrhage (*stars*) and tumor cells (*arrow*) in the stroma.

Minor salivary glands follow in frequency, especially in the palate (21%).[12,13] According to a well-documented series, MEs are less prone to recur than pleomorphic adenomas.[14] In our cases, 1 of 10 tumors was a recurrence. Recurrence is correlated with positive margins at the first excision.[15] The recommended treatment is complete surgical excision. Benign MEs can undergo malignant transformation, especially in long-standing tumors or in tumors with multiple recurrences.[16]

Imaging features of ME are rarely reported in the English literature because of their low prevalence. Our study showed that 9 tumors were located in the superficial lobe of the parotid gland, 1 was located in the tail of parotid gland, and all of the tumors abutted the capsule of the gland. Two cases showed homogenous enhancement. The remaining 8 cases demonstrated inhomogeneous enhancement with enhancing nodules, the presence of cystic areas in 3 tumors (Fig 2), slitlike-shaped area in 3 tumors (Fig 3), and linear bands in 2 tumors (Fig 4).

By correlating the CT appearances and the microscopic specimens, we concluded that the enhancing nodules on CT were most probably due to epithelial nets with plentiful blood vessels and that nonenhancing linear bands on CT were most probably due to either collagenous or mucoid stroma. Also, we postulated that the slitlike-shaped nonenhancing area might correspond with stroma surrounding hemorrhage.

From the standpoint of the CT scan findings, the most important differential diagnoses for ME of the parotid gland include benign pleomorphic adenoma and Warthin tumor. The CT features of these 2 more common tumors have been described in detail in the literature. Pleomorphic adenomas show little or no enhancement in the immediate postcontrast scan but manifest increased enhancement in the delayed scan.[8,9] In addition, pleomorphic adenomas could happen in superficial and/or deep lobes of the parotid and not often abut the capsule of the gland. Relatively large cystic changes were seen in 3 of 10 tumors in our study (Fig 2). These changes are more frequent in MEs than in pleomorphic adenomas.

Warthin tumors show enhancement in the immediate postcontrast scan.[9] These features are similar to MEs; however, radiologic demonstration of enhancing nodules forma-
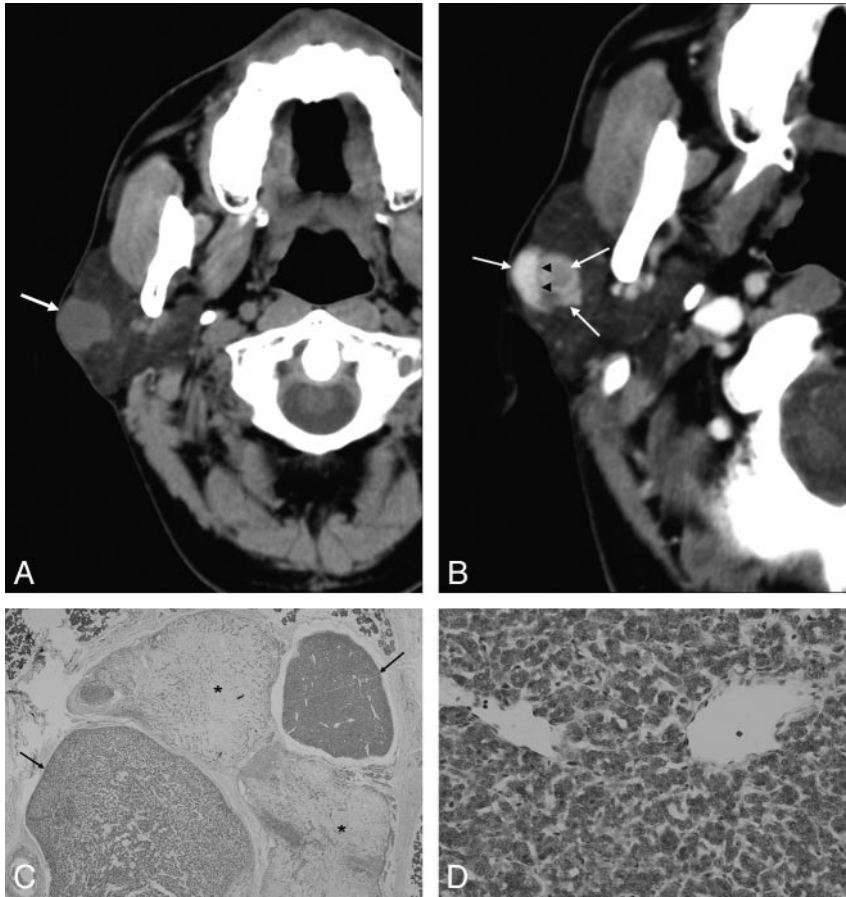
Fig 4. A 54-year-old man with ME. *A,* Precontrast axial CT scan shows a well-defined mass with a lobulated margin in the superficial lobe of the right parotid gland abutted on the capsule of the gland (*arrow*). *B,* Contrast-enhanced axial CT scan shows the mass with inhomogeneous enhancement. It contains enhancing nodules (*arrows*) and nonenhancing linear band (*arrowheads*). *C,* Microscopic examination (HE; ×2) shows the stroma (*black asterisks*) and epithelioid nests (*arrows*) with a lot of vessels. *D,* Microscopic examination (HE; ×100) shows that the nest is composed of plasmacytoid.

tion is more common in MEs, and lobulated contours were seen in half of the cases in our study and are more frequent in MEs than in Warthin tumors. Moreover, Warthin tumor is more common in elderly men than in women and can be multifocal and bilateral in 10%–15% of patients.[17,18] In addition, parotid scintigraphy by using technetium Tc99m-pertechnetate is useful for the diagnosis of a Warthin tumor.[19] Low-grade malignant tumors usually demonstrate similar CT findings to benign tumors. Imaging findings are usually nonspecific and indistinguishable from those of benign parotid tumors.

Conclusions

CT imaging findings of MEs were well circumscribed, enhancing mass lesions with smooth or lobulated margins, located chiefly in the superficial lobe and abutted on the capsule of the gland. They may contain enhancing nodules and nonenhancing areas of linear bands, slitlike-shaped or of cystic configuration. Although MEs are a rarity, they should be suspected when a tumor shows all of the characteristics noted here.

References

1. Barnes L, Eveson JW, Reichart P, et al. *World Health Organization Classification of Tumours. Pathology and Genetics of Head and Neck Tumours.* Lyon, France: IARC Press; 2005:259
2. Ellis GL, Auclair PL. **Tumors of the salivary glands, third series, Fascicle 17.** In: *Atlas of Tumor Pathology.* Washington, DC: Armed Forces Institute of Pathology; 1996:80–94
3. Bryan RN, Miller RH, Ferreyro RI, et al. **Computed tomography of the major salivary glands.** *Am J Roentgenol* 1982;139:547–54
4. Casselman JW, Mancuso AA. **Major salivary gland masses: comparison of MR imaging and CT.** *Radiology* 1987;165:183–89
5. Sone S, Higashihara T, Morimoto S, et al. **CT of parotid tumors.** *Am J Neuroradiol* 1982;3:143–47
6. Golding S. **Computed tomography in the diagnosis of parotid gland tumors.** *Br J Radiol* 1982;55:182–88
7. Silvers AR, Som PS. **Salivary glands.** *Radiol Clin North Am* 1998;36:941–66
8. Lev MH, Khanduja K, Morris PP, et al. **Parotid pleomorphic adenomas: delayed CT enhancement.** *AJNR Am J Neuroradiol* 1998;19:1835–39
9. Choi DS, Na DG, Byun HS, et al. **Salivary gland tumors: evaluation with two-phase helical CT.** *Radiology* 2000;214:231–36
10. Jang M, Park D, Lee SR, et al. **Basal cell adenoma in the parotid gland: CT and MR findings.** *AJNR Am J Neuroradiol* 2004;25:631–35
11. Seifert G, Sobin LH. **Histological typing of salivary gland tumors.** In: *World Health Organization International Histological Classification of Tumors,* 2nd ed. Berlin, Germany: Springer-Verlag; 1991:20–21
12. Barnes L, Appel BN, Perez H, et al. **Myoepithelioma of the head and neck: case report and review.** *J Surg Oncol* 1985;28:21–28
13. Waldron CA. **Mixed tumor (pleomorphic adenoma) and myoepithelioma.** In: Ellis GL, Auclair PL, Gnepp DR, eds. *Surgical Pathology of the Salivary Glands.* Philadelphia: WB Saunders; 1991:165–86
14. Sciubba JJ, Brannon RB. **Myoepithelioma of salivary glands: report of 23 cases,** *Cancer* 1982;49:562–72
15. El-Naggar A, Batsakis JG, Luna MA, et al. **DNA content and proliferative activity of myoepitheliomas.** *J Laryngol Otol* 1989;103:1192–97
16. Alos L, Cardesa A, Bombi JA, et al. **Myoepithelial tumours of salivary glands: a clinicopathologic, immunohistochemical, ultrastructural and flow cytometric study.** *Semin Diagn Pathol* 1996;13:138–47
17. Howlett DC, Kesse KW, Hughes DV, et al. **The role of imaging in the evaluation of parotid disease.** *Clin Radiol* 2002;57:692–701
18. Eveson JW, Cawson RA. **Salivary gland tumors: a review of 2410 cases with particular reference to histological types, site, age and sex distribution.** *J Pathol* 1985;146:51–58
19. Miyake H, Matsumoto A, Hori Y, et al. **Warthin's tumor of parotid gland on Tc-99m pertechnetate scintigraphy with lemon juice stimulation: Tc-99m uptake, size, and pathologic correlation.** *Eur Radiol* 2001;11:2472–78